Experimental Device for Simulating Traumatic Brain Injury Resulting from Linear Accelerations

Michael D. Gilchrist

Department of Mechanical Engineering
University College Dublin
Belfield, Dublin 4, Ireland

Michael.Gilchrist@ucd.ie

ABSTRACT

Various methods are used to model and analyse traumatic brain injuries (TBI) in the human. These include volunteer and cadaver experiments, anthropomorphic dummies, physical models, computational models and mathematical models. The pathophysiological response to mechanical impact of the human central nervous system and of *in-vivo* neural tissue is most realistically analysed using animal models, which provide the best surrogate for the human brain. During non-fatal impacts, a mechanical insult may trigger a cascade of physiological processes, many mediated by neurochemicals within the neural tissue which will, in turn, control the depth and extent of the brain injury. This present paper reports the development of a novel experimental device which can apply different linear acceleration impacts directly to *in-vivo* neural tissue in a manner which permits the experimental analysis of non-fatal TBI of varying severity.

KEYWORDS

Traumatic brain injury (TBI), tissue damage, linear acceleration, impact biomechanics, experimental device

TERMINOLOGY

acute	having a sudden onset, sharp rise, and short duration (Vs. chronic which lasts a long time)
arachnoid	a thin membrane of the brain and spinal cord that lies between the dura mater and the pia mater
axon	a usually long and single nerve cell process that usually conducts impulses away from a cell body
basal ganglia	the four deeply placed masses of grey matter within each cerebral hemisphere, namely the caudate nucleus, the lentiform nucleus, the amygdala, and the claustrum
brain stem	the part of the brain composed of the midbrain, pons, and medulla oblongata and connecting the spinal cord with the forebrain and cerebrum
calvarium	the portion of the skull including the brain case but excluding the lower jaw and facial portion

cerebellar peduncles	three large bands of nerve fibres that join each hemisphere of the cerebellum with the parts of the brain below and in front, namely (i) the superior cerebellar peduncle joins the cerebellum wit the midbrain, (ii) the middle cerebellar peduncle connects the cerebellum with the pons and (iii) the inferior cerebellar peduncle connects the cerebellum with the medullar oblongata and the spinal cord
cerebellum	a large dorsally projecting part of the brain concerned especially with the coordination of muscles and the maintenance of bodily equilibrium, situated between the brain stem and the back of the cerebrum and formed of two lateral lobes and a median lobe
cerebral cortex	the surface layer of grey matter of the cerebrum that functions chiefly in coordination of sensory and motor information
concussion	a jarring injury of the brain resulting in disturbance of cerebral function and sometimes marked by permanent damage
contusion	injury to tissue without laceration (e.g., bruise)
corpus callosum	the great band of commissural fibres uniting the cerebral hemispheres
cortex	the outer layer of grey matter of the cerebrum and cerebellum
craniotomy	surgical opening of the skull
cranium	that part of the skull enclosing the brain
cytoskeleton	the network of protein filaments in the cytoplasm that controls cell shape, maintains intracellular organisation, and is involved in cell movement
dorsolateral quadrants/region	of, relating to, or involving both the back and sides
dura or dura mater	the tough fibrous membrane that envelops the brain and spinal cord external to the arachnoid and pia mater, that in the cranium closely lines the bone, does not dip down between the convolutions, and contains numerous blood vessels and venous sinuses, and that in the spinal cord is separated from the bone by a considerable space and contains no venous sinuses
extradural (epidural)	location that is on or outside the dura mater but within the skull
foramen magnum	the opening in the skull through which the spinal cord passes to become the medulla oblongata
grey matter	neural tissue of the brain and spinal cord that contains cell bodies as well as nerve fibres, has a brownish grey colour, and forms most of the cortex and nuclei of the brain
haematoma	a mass of usually clotted blood that forms in a tissue, organ, or body space as a result of a broken blood vessel

haemorrhage	a copious discharge of blood from the blood vessels
hernia	a protrusion of an organ or part through connective tissue or through a wall of the cavity in which it is normally enclosed
in-vitro	in an artificial situation
in-vivo	in a real-life situation
intracerebral haematoma	haematoma within the cerebrum
intracranial haematoma	haematoma within the cranium
lesion	an abnormal and well defined change in structure of an organ or part due to injury
medulla oblongata	the pyramidal last part of the brain which is continuous posteriorly with the spinal cord and encloses the fourth ventricle
meninges	the three membranes that envelop the brain and spinal cord, namely, the arachnoid, dura mater and pia mater
organelle	a specialised cellular part that is analogous to an organ
parasagittal veins	veins situated alongside of or adjacent to a sagittal location or sagittal plane
pia or pia mater	the delicate and highly vascular membrane of connective tissue investing the brain and spinal cord, lying internal to the arachnoid and dura mater, dipping down between the convolutions of the brain
pons	a broad mass of chiefly transverse nerve fibres conspicuous on the ventral surface of the brain and the anterior end of the medulla oblongata
rostral	situated towards the oral or nasal region
splenium	the thick rounded fold that forms the posterior border of the corpus callosum
subarachnoid	situated or occurring under the arachnoid membrane
subdural haematoma	a haematoma that occurs between the dura mater and arachnoid in the subdural space and that may apply neurologically significant pressure to the cerebral cortex
white matter	neural tissue that consists largely of myelinated nerve fibres, has a whitish colour, and underlies the grey matter of the brain and spinal cord

1 INTRODUCTION

Mechanical impacts to the head are described as non-invasive (non-penetrating), or invasive (penetrating) whilst head injuries can result from direct and indirect impact events. Loading durations to the human head are classified as static (> 200 ms) or dynamic (< 200 ms) [1]; these time durations require scaling for application to an animal model. Direct impact (i.e. full-contact) is associated with contact phenomena (local disturbances at the site of impact: fracturing, fragmentation, penetration, perforation), and the initiation and propagation of transient stress waves (dilational, shear, compressive) in the intracranial tissues and skull [2]. The significance of these effects will depend on the constitutive properties of the cranial and

intracranial tissues. The contact forces that are produced when the head is struck by, or strikes, a hard object often produce focal effects alone. However, under certain conditions these contact loads will accelerate rapidly and/or decelerate the intracranial contents, inducing inertial forces throughout the brain [3].

The geometry and momentum of the impacting body is also critical to the degree and type of injury sustained. Gennarelli [4] explains that a small, high-velocity object will cause little movement and thus kinetic energy is dissipated through contact phenomena. On the other hand, a large blunt object acts to accelerate the head, with less severe contact effects. The actual movements of the brain during a blunt impact will, therefore, be influenced by the magnitude and direction of the applied force. It is also influenced by the presence of anatomical morphology such as the foramen magnum, and the elastic deformation of the skull in the area of the blow [5].

Indirect impact (i.e. non-contact), also described as impulsive or inertial loading, rapidly accelerates the skull – brain system under translation and/or rotation. This is the first stage of a sequence of events that will initiate a response to mechanical impact [6]. Inertial loading due to indirect impact normally leads to an injury when the impact duration is more prolonged. However, the rate of acceleration onset, which determines the rate at which the inertial forces deform the brain tissue and is hence proportional to the strain rate is critical. The type and degree of injury sustained by inertial loading are therefore a function of the rate of acceleration onset, the duration of acceleration, the peak acceleration, and the plane of rotation.

Due to its inertia, the brain resists simultaneous rotation with the skull. It has been shown by numerous studies that the brain lags the skull [7]. In this way, the degree to which head motion is restricted is also of importance in determining the relative contributions of impact and inertial components in head trauma. No matter which mechanism of impact is applied, the impact and inertial components will both culminate in tissue strains. Those tissues most at risk are the vascular and neuronal tissues. As the impact duration increases, the relative amount of tissue strain due to impact effects is shown to decrease, while the tissue strain due to inertial effects becomes more dominant [8]. As with any structural material, tissue deformations will manifest as compressive, tensile and shearing strains.

The ratio of the duration of loading to the natural period (= inverse of natural frequency) of the brain structure (approximately 30 to 100 ms for animals and humans [9]) can also indicate the magnitude of internal displacement and the degree of damage due to tissue strain. Certain parameters, including impulse and average or peak applied force, can be identified from this ratio. In this regard, the natural frequency of an animal model's brain should be determined for inertial impact studies.

- Ratio < 1: the same impulse and duration will result in the same injury, even if the maximum force/acceleration varies over a wide range, i.e., the impact event has concluded before the structure reacts.
- Ratio > 1: the same maximum force/acceleration will result in the same injury, even if the impulse and duration will vary over a wide range.
- Ratio ~ 1: neither the impulse or maximum force/acceleration alone can characterise the sensitivity and the entire force-time function must be considered [9].

In brief, the shorter the duration of loading, the greater the acceleration required for the same velocity response. Fig. 1 illustrates how increasing the impact duration affects the peak acceleration that is necessary to induce a given amplitude response.

Any trauma to the head which involves the scalp, skull or brain can be considered to be a head injury. In clinical practice these injury groups often occur together [10]. While each group of injuries should be included in a full biomechanical analysis, the application of the present work is concerned principally with brain injuries and associated lesions. To distinguish from the general term of head injury, it is convenient to define traumatic brain injury (TBI) as any damage affecting brain function and resulting from non-penetrating head loading, either of the contact or the non-contact type. The two main groups of lesions which result from dynamic loading of the brain are called focal and diffuse. Brain injuries are also further classified as primary and secondary.

Focal Injuries

Focal brain injuries are described by primary localised tissue damage. In severe cases, if the lesion is sufficiently large, they can result in coma due to brain shift, herniation and brain stem compression [11]. The main types of focal injury are primary brain contusions and intracranial haematomas.

Several types of primary brain contusion (bruising) can occur, depending on the location and degree of impact [12]. A cortical brain surface contusion is described by haemorrhages in the cerebral cortex, often coupled with focal subarachnoid haemorrhaging. Cortical-subcortical contusions result from any combination of frontal, parieto-temporal or occipital impacts and in some cases can be related to the mechanism of coup ('ipsilateral to impact') and/or contrecoup ('contralateral to impact') rebounding of the brain within the cranial vault.

In clinical neurosurgical practice, intracranial haematomas are most often classified by the immediate physiological spaces which are occupied by extravasated blood (e.g., extradural, subdural, subarachnoid, intraventricular, and intraparenchymal lesions – in so far as can be delineated by CT scanning). It is important to note that an intracranial haematoma may in fact belong to more than one of these categories; such lesions are often further characterised by regional localisation (e.g., frontal, temporo-parietal, occipital, infra-tentorial) and also by chronicity (e.g., acute, sub-acute, acute-on-chronic, chronic, etc.). Intracranial haematomas clearly result from rupturing of the vascular tissues, and as a result, volumes of extravasated blood may lead to a disturbance of neurological function. Clincally siginifcant traumatic extradural (epidural) haematomas occur on, or over, the dura mater, and are most often caused by injury to the meningeal arterial vessels, and less commonly by injury to meningeal venous vessels, skull fracture (i.e., fracture haematoma), or tearing of dural venous sinuses. Acute subdural haematomas (ASDH) are clinically the most lethal focal lesion [13], and can be of arterial or venous origin. This type of haematoma results from primary damage to the surface blood vessels.

Traumatic, clinically significant ASDHs may occur in the following contexts: (i) direct laceration of the cortical arteries and veins (e.g., as per penetrating injuries), (ii) closed injuries resulting in large contusions which cause bleeding into adjacent subdural space, and (iii) tearing of the parasagittal veins that bridge the subdural space.

In general, particularly in young patients, ASDHs occur due to vascular injury caused by relatively short duration rotational acceleration loading at high acceleration rates, for example falls or impact on firm, unyielding surfaces [4]. However, Gennarelli and Thibault [8] showed that ASDH can occur without the head being struck, i.e., by indirect acceleration. Although impact to the head is the most common cause of clinical ASDH, it is the

acceleration induced by the impact, and not the head contact itself that causes this type of lesion. This is due to the fact that impact conditions are associated with high strain-rate conditions. The purest form of ASDH without head impact often results from the violent shaking of infants. An experimental model of ASDH has shown that rupturing of the bridging veins occurs due to their strain-rate sensitivity [8]. The results of this model were consistent with the clinical causes of ASDH, where three quarters of a population of patients with ASDH were due to high strain-rate falls and assaults and one quarter were due to lower strain-rate vehicular injuries.

Diffuse Injuries

These injuries result from the bulk mechanical effects associated with axonal, neural, microvascular and brain swelling injuries. They occur under distributed loading conditions which generally induce relatively low energy damage, affecting a multitude of distinct regions of neural tissue. The most common of these is described by a distribution of focal lesions in the axonal components of the neural structure. Such widespread axonal damage has come to be known as diffuse axonal injury (DAI). In comparison with the conditions required for ASDH, DAI injuries require a lower rate of acceleration onset, but a more prolonged impact duration. They are associated with widespread primary brain damage during which shearing of the axonal tissue occurs. Although the formation of DAI is produced by inertial forces, contact forces often cause the levels of acceleration necessary to produce DAI. Axonal injury is therefore dependent on both the magnitude of strain and the rate of strain during the brain trauma event.

An important difference between focal and diffuse brain injury is the source and character of post-traumatic coma resulting from these two general forms of injury. Focal brain injury may include mass effects from a haemorrhagic contusion or haematoma, which can induce herniation and brain stem compression. Consequently, a resultant coma may not be immediate but may develop in a secondary fashion. In the case of DAI, non-impact rotational acceleration can induce an immediate and prolonged post-traumatic unconsciousness in the absence of mass lesions.

Nishimoto and Murakami [14] report that, based on their computational analysis, DAI may occur by rotational acceleration, as well as by direct impact with pure translational acceleration. They also argue that the occurrence of DAI is not influenced by the acceleration of rotational or translational impacts to the head, but rather that the concentration of shear stress at the core of the brain, due to the effects of the internal head structures, is the mechanism of DAI. Adams et al. [15] describe three severity grades of DAI. Grade I is characterised by axonal injury in the white matter of the parasaggital cerebral hemispheres, corpus callosum, brain stem and cerebellum, Grade II by focal lesions in the corpus callosum, and Grade III by additional focal lesions in the dorsolateral quadrants of the rostral brain stem, particularly in the superior cerebellar peduncles.

Recent biomechanical studies by Smith and Meaney [3] give a comprehensive description of what is now understood to be the mechanism of DAI. The susceptibility of the axons to mechanical injury appears to be due to both their viscoelastic properties and their highly organised structure in the white matter tracts. Although axons are supple under normal conditions, they behave in an inelastic manner when exposed to rapid deformations associated with brain trauma. Accordingly, rapid stretch of axons can damage the axonal cytoskeleton, resulting in a loss of elasticity and impairment of axoplasmic transport. Subsequent swelling of the axon occurs in discrete bulb formations or in elongated

varicosities that accumulate 'organelles'. Ultimately, swollen axons may become functionally or anatomically disconnected from their existing networks [16] and contribute to additional neuropathologic changes in brain tissue.

Although termed 'diffuse', the pattern of axonal damage in the white matter is more accurately described as 'multifocal' [3], appearing throughout the deep and subcortical white matter, and is particularly common in midline structures, including the splenium of the corpus callosum. In mild to low/moderate DAI, there is often an absence of macroscopic pathology and the brain may appear normal upon radiological examination (i.e., CT scanning). Nevertheless, microscopic examination of the brain tissue reveals the pathologic signature of DAI: a multitude of swollen and disconnected axons. In high severity DAI, the axonal pathology is accompanied by tissue tears in the white matter with intraparenchymal haemorrhage usually located centrally in the corpus callosum, basal ganglia, and dorsolateral region of the rostral brainstem. This level of DAI is associated with prolonged unconsciousness, high mortality, and poor outcome in survivors.

The present paper reviews the range of experimental models which have been used to induce and to characterise traumatic brain injuries. These various models have tended to be developed from a biomechanical perspective, i.e., whether an impact injury resulted from either translational and/or rotational accelerations. The experimental device described in this paper has been developed to apply a translational impact directly to the brain surface. Experimental models can be graded according to their behavioural, pathological, physiological, and biochemical fidelity to human brain injuries. Within the context of the present head impact biomechanics research activity, it is ultimately intended that this device will be used in conjunction with neurochemical microdialysis techniques as a model to analyse non-fatal TBI. Such an experimental approach will complement computational mechanics analyses [17-22] of neurotrauma.

2 REVIEW OF EXPERIMENTAL MODELS OF HEAD INJURY

The biomechanics of intracranial injuries [10, 23], and the suggested experimental procedures to reproduce them, are well documented in the literature. However, no standardised mechanical test procedure exists for conducting such experiments and the specific technical details pertaining to the various devices used in these experiments are seldom available in publicly available literature. In some cases, this makes it difficult to critically judge the reliability of certain methods. Experimental fixtures have been developed to use gases, liquids and rigid-bodies as impacting media. These test devices are divided between those that apply impact directly to the brain in an invasive manner after a craniotomy ('direct brain impact models'), and those that induce acceleration of the intracranial contents by impacting the exterior of the head itself ('direct head impact models'). Furthermore, inertial methods that allow translational and/or rotational acceleration of certain animal models by indirect impact have also been designed, although these will not be discussed in this present paper.

Direct Brain Impact Models

Rigid-Body Impact Devices

Simple weight-drop methods have been used [24] to produce direct focal cortical compression of the exposed dura. However, due to the variation of impact velocity by the

falling impactors, the biomechanical data fails to accurately describe the resulting brain deformations. Koizumi et al. [25] produced a cerebral contusion in the right parietal cortex by a weight-drop method which incorporated the use of microdialysis, as illustrated in Fig. 2. The height for the weight drop was optimised prior to the experiment, by reference to the resulting physiological responses (i.e., certain responses were not observed when the lead weight was dropped on the aluminium impactor from heights of 0.3, 0.6 or 0.9 m). Shear-induced damage of the neural tissue was avoided by removing the implanted microdialysis probes from the brain just before dropping the weight, and by replaced these at the same stereotaxic positions within 30 s of the insult.

Controlled cortical impact (CCI) is an invasive impact method that was first proposed by Lighthall [26] after adapting similar methods used in spinal cord contusion experiments [27]. Lighthall's original system was used to impact the intact dura mater of a ferret by means of a stroke-constrained pneumatic cylinder and piston with a hemispherical aluminium impactor tip (6.25 mm radius) which were rigidly mounted on an adjustable (variable angle and position) vertical crossbar. By varying the air pressure [28], contact velocities ranged from 0 – 4.0 ms^{-1}, with 2.0 – 5.0 mm deformations.

Many others have adopted this method by designing similar systems [29, 30], including Cherian et al. [31], who used an 8 mm diameter impactor tip, which penetrated either 2, 2.5, or 3 mm into the dura, as shown in Fig. 3. Similar size pneumatic cylinders were used in all cases. Variations in the geometry, shape and material of the impactor tip were encountered in all published descriptions.

Vacuum Deformation Devices

Dynamic cortical deformation (DCD) is an invasive method developed by Shreiber et al. [32, 33], based on earlier work by Murai et al. [34]. It involves rapidly deforming the exposed cerebral cortex by a 'transient, non-ablative vacuum pulse' which causes local tensile loading of the meninges. The device allows independent control of the magnitude, duration, and shape of the vacuum pulse. The mechanical response of the cortex is measured non-invasively via a calibrated laser displacement transducer positioned above the exposed cortex.

Shreiber et al. [33] applied negative pressures of 13.8, 20.7 and 27.6 kPa (= 2, 3, and 4 psi) for 25, 50 and 100 ms durations. These conditions resulted in graded, localised, focal cerebral lesions, mimicking the rapid tissue deformation that occurs during TBI. Damage was confined to the region immediately surrounding the applied mechanical loading. The authors claim that the consequences of cerebral contusions could be examined in isolation from other brain injuries. They also emphasised the fact that this type of localised cortical damage could be produced by other methods including ablation [35] and freezing.

Inadequacies encountered with this method included a slight lagging of displacement with applied vacuum pressure, as well as permanent displacement of the cortex. A linear regression analysis showed that the displacement was significantly related to the vacuum pressure.

Mathew et al. [35] have also produced highly focal lesions in the rat brain by applying a long-duration (5 s) vacuum pulse to the intact dura. This method of ablation also restricts the injury area. However, the ablation method used in their work seems to lack measurement accuracy when compared with similar systems. This design of the suction apparatus was very simple, and consisted of a syringe filled with normal saline, primed to deliver a constant

negative pressure. In a revised study of their model, Mathew et al. [36] explained that, in comparison, impact and inertial injuries produce variable lesions associated with widespread axonal damage. Percussion and acceleration methods therefore produce a complex mixture of focal and diffuse damage, complicated by interdependent physiological responses. Also, cortical impact and weight drop methods both produce cortical damage with variable lesions.

Fluid Impact Devices

Fluid percussion was first reported by Lindgren and Rinder [37], for use in a rabbit model. This invasive method involves injecting fluid (saline or blood) into the epidural, subdural, or intracerebral compartments, as shown schematically in Fig. 4. It has proven useful for producing graded injury responses systematically and centrally, and has been modified [38-41] and widely applied to many other animal models (dog, rabbit, cat, swine, rat).

Yamaki et al. [42] used a modified version of the midline and lateral fluid percussion method to induce graduated levels of brain injury in a rodent model, by rapidly injecting saline into the closed brain cavity. Axonal injury and contusions were produced. Changes in the stiffness of the Plexiglas tube due to changes in temperature, and air bubbles in the reservoir, were seen to affect the fluid percussion force. Pressure pulses were measured by varying the fluid volume in the reservoir and the amplitude of the impacting pendulum, as shown in Fig. 5. The effect of air bubbles in the cylinder was measured by locating the transducer close to the fluid-flushing outlet and piston. The volume of the reservoir was also controlled by using two cylinders (15º to horizontal) with different external diameters. By improving the position of the pressure transducer and structure of the fluid cylinder, this modified device was capable of generating an accurate pressure pulse and accurately measuring the wave characteristic. The saline reservoir volume and pendulum height could be varied simultaneously to produce a wide range of pressure pulses. However, the pressure characteristic and waveform are still not a direct index of mechanical influence to the brain. The mechanism of injury by fluid percussion is dissimilar to the closed-head injury in humans, in which injury results from impacting skull with acceleration-deceleration movement of the brain.

It has also been shown [28] that the fluid percussion pulse produces a complex, diffuse and dynamic pattern of loading in the intracranial contents, with a continuously changing wavefront. Also, because fluid is used to transfer mechanical energy to the brain tissue, and because fluid flow characteristics (direction, displacement and velocity) are dependant on the brain geometry and species used, accurate analytical and biomechanical analyses of the resultant injury would be difficult at best. Consequently, this method is not ideally suited for detailed biomechanical analysis.

Direct Head Impact Models

A series of classical experiments by Denny-Brown and Russell [43], that applied direct-impact to the unrestrained head of animal models, laid the basis for many subsequent methods. In their studies, restraint was only provided by the neck, which resulted in complex and ill-characterised three-dimensional movements. It was observed that by unrestraining the cranium, the occurrence of concussion from impact was increased. Although some studies using unrestrained methods have attempted to evaluate the effects of rotational and translational acceleration separately, careful biomechanical analysis of the experiments clearly shows that skull impact produces both rotational and translational acceleration

components in all cases [28]. Furthermore, full head constraint is not easily obtained during impact events.

Direct head impact experiments have primarily involved pistons [44, 45] and drop-weights [46-51]. Impact is applied directly to the cranium, which may be protected by a metallic plate to distribute loading and prevent skull fracture. Unprotected direct impact to the rat model results in either no change, or dramatic changes, due to the rat's extremely steep injury tolerance curve. Therefore, even a slight change in the impact parameters may change the injury outcome from minor to fatal [44]. These methods have therefore not been successful at producing a spectrum of clinically relevant injury in the rat. The occurrence of skull fracture from impact is not well correlated with injury in the rat model [28]. Direct cranial impact methods therefore have a high degree of variability in the response. This result stems from a lack of control over the precise conditions of impact, the dynamic response of the head, and inconsistent parameters at the impactor-skull interface.

Many other less-conventional devices have been used to experimentally reproduce traumatic brain injury in animal models. These include lead-tipped darts [52], bolts [53], pendulum devices [54], and padded darts fired from pistols [55].

3 DEVELOPMENT OF LINEAR ACCELERATION IMPACT RIG

It was decided to develop a linear impact rig which was functionally similar to the controlled method of impact developed by Dixon et al. [29] and Cherian et al. [31]. Gas and fluid impact methods were considered to be incompatible with the neurochemical analysis technique of intracerebral microdialysis, and would introduce complex impact conditions upon the neural tissue (i.e. turbulent fluid effects). The system was designed to apply a rigid-body impact directly to the exposed cortical surface. The line of action of the impact passed through the centre of mass of the brain and thus rotational acceleration effects were avoided. The following requirements were considered necessary:

- variable impact position (i.e. frontal, temporal) and deformation distance to be applied accurately and repeatedly,
- robust frame to accommodate a stereotaxic unit for *in-situ* microdialysis measurements of different neurochemicals, and
- minimal instrumentation to be used due to constraints of limited laboratory space.

Figure 7 provides a detailed view of the impact rig including the attached stereotaxic frame. A double-actuated pneumatic actuator (20 mm bore diameter, 8 mm connecting rod diameter, 125 mm stroke length, Bimba Company Model Number EM-25-50-N) was used to control the high-speed linear motion of the impactor tip. This was more convenient to use in a laboratory environment than an electrical actuator. The effective area of the actuator on the out stroke was 314 mm^2 and 264 mm^2 on the in stroke. The thrust force applied on the out stroke, i.e., during an impact experiment, varied linearly with the gauge pressure of the compressed air: the range of pressures and forces which were within the capacity of this system are given in Table 1. This corresponded to a maximum static equilibrium force of approximately 200 N under a continuous pressure of 650 kPa (= 6.5 bar).

Pressure [kPa]	200	250	300	350	400	450	500	550	600	650
Equilibrium	62.80	78.50	94.20	109.90	125.60	141.30	157.00	172.70	188.40	204.10

Force [N]										

Table 1: Theoretically predicted variation of quasi-static equilibrium force with air pressure for actuator used in impact rig.

Clearly with this present design and actuator, it is possible to apply significant forces (> 200 N) during an impact experiment. The rate of strain within the impacted neural tissue will depend on the impact velocity of the piston, which is a function of the circuit volumetric flowrate and the flow restrictions within the actuator. Since any mechanical disturbance of the cortical surface will likely cause some form of underlying cellular response, this system was considered to be appropriate to analyse non-fatal TBIs.

Four electromechanical reed switches, connected in parallel, were physically positioned at different locations along the cylinder casing of the actuator, in line with the stroke direction. Therefore, as the actuator piston moves along the stroke, each switch closes (on) and re-opens (off) in turn, once the magnet attached to the head of the actuator has passed. The circuit box was fitted with outlets connected across the load (resistor), and fed to a storage oscilloscope. Therefore, as the piston completes the out stroke, a discrete digital signal is captured on the oscilloscope screen, in the form of a clean square wave. The time interval between each switch's activation can then be recorded directly. Given that the relative locations of the switches are known, the velocity of the piston is easily calculated for specific locations along the cylinder. In terms of the impact experiments, only the velocity at the end of the stroke (i.e., impact velocity) needs to be determined. The other reed switches allow the velocity to be measured prior to impact, and thus to ensure that the velocity of the piston is linear at the end of the stroke (i.e., the actuator is not accelerating). The velocity measurements were systematically calibrated to ensure that the impact velocity remained consistent with the range of air pressures used and were also constant throughout the final 15 mm travel of the stroke. From this calibration analysis, it became clear that the actuator quickly accelerates at the beginning of the stroke, and that the velocity is constant (1.250 ms^{-1} for a gauge pressure of 600 kPa) towards the end of the stroke. The process was repeated, and verified for a range of air pressures. Table 2 summarises the measured dependence of impact velocity with the gauge pressure of the air.

Pressure [kPa]	150	200	250	300	350	400	450	500	550	600	650
Velocity [ms^{-1}]	0.938	1.071	1.119	1.154	1.172	1.190	1.210	1.230	1.246	1.250	1.250

Table 2: Calibrated measurements of impact velocity with gauge pressure.

The frame of the impact test rig was machined from mild steel in order that it would be sufficiently robust to allow the linear actuator to be held securely in a range of adjustable positions, representing various angles of impact. The frame also had to accommodate the stereotaxic unit and the ear bars so that the centroid of the rat's head would be maintained at a constant height of 64 mm above the datum. To ensure repeatability of experiments, it was also necessary that the structure would remain rigid and stable relative to the laboratory work surface. The design incorporates a pivot, which can rotate through 90º whilst a mounting bracket allows the actuator to be positioned at any point along a pivoted arc, as seen in Fig. 7. Thus, any angle in a quarter-sphere can be chosen, and will always be equidistant from the target point, located 64 mm above the datum. The manner in which the impactor can be

rotated about two axes provides complete flexibility to vary the line of action of the impactor while still ensuring that the impact has no component of rotational acceleration: this is more versatile than the impact device of Cherian et al. [31].

The theoretical static force exerted by the piston can be determined from the static pressure readings (Table 1). The static force is the equilibrium force exerted on the piston (and by the piston on the load) once the pressure in the circuit has equalised. Initially, as the solenoid controlling the air flow in the actuator cylinder is opened and the flow of air passes through the circuit to the cylinder, a variation in pressure is observed as the flow meets restrictions in cross sectional area. The time taken for the pressure (i.e., the force of the air on the piston) to equalise would be reflected in a velocity-time (acceleration) profile of the piston rod, and by a force-time profile at impact. Furthermore, inertial forces on the piston act to positively accelerate the piston as it gathers momentum towards the end of the stroke. This superimposed force component partially compensates for the time lag in pressure equalisation. The inertial force exerted by the piston can be determined by applying Newton's second law for a moving body. Given that the velocity of the piston is known at impact (Table 2), the inertial force can be determined if the total mass of the moving bodies (piston + piston rod + aluminium impactor tip) is also known. The total mass of the moving bodies is calculated from the pneumatic component data sheets (Bimba Company), and from the known mass of the hemispherical aluminium impactor tip (0.004kg ± 5%). It is clear that for small masses, the inertial force will be small in comparison to the static force, upon which it will be superimposed. For accurate calculations of the total impact force, the inertial force must be considered. For example, the total impact force can be analytically determined from the following results recorded at 600 kPa (6.0 bar) gauge pressure:

Impact velocity, $V = 1.250\ ms^{-1}$

Average acceleration of stroke, $a_{avg} = \Delta V/\Delta t = 1.250/0.117 = 10.684\ ms^{-2}$

Mass of piston and piston rod = 0.150 + (0.0008 * 125) = 0.250 kg

Total mass includes impactor tip = 0.004 + 0.250 = 0.254 kg

$F_{Inertia} = (0.254 * 10.684) = 2.714$ N

Hence, the maximum impact force that can be expected at a gauge pressure of 600 kPa (6.0 bar) is calculated analytically as:

$F_{Total\ Impact\ Force} = F_{Inertia} + F_{Static} = 2.714 + 188.40 = 191.11$ N

These theoretical calculations of the impact force were separately verified by attaching the actuator and air-pressure system to an instrumented load cell. It was specifically decided not to integrate a load cell with the test fixture for *in-situ* use within a laboratory environment in order that a minimum amount of instrumentation would be incorporated into the impact rig. Figure 8 presents the variation of dynamically measured force during these verification tests for a gauge pressure of 600 kPa: experimentally measured static and inertial forces were 185.2 N and 2.7 N, respectively. The results from these validation measurements are within 1.5% of those predicted theoretically and we can therefore conclude that:

- The inertial force measured experimentally is the same as that predicted analytically as being $F_{Inertia} \approx 2.7$ N. This was found to be true for all pressures (100 – 700 kPa).

- The error in the measurement of static force is less than 1.5%.

This validation procedure was repeated for a range of alternative pressures between 150 and 650 kPa, the results of which indicated that as the pressure is increased:

- The slope (rate of force application) of the response increases, reflecting the increased impact velocity and volumetric flowrate of the pneumatic system.
- The impact force is linearly proportional to the increase in pressure, where the effective piston area is the coefficient of proportionality.

In each case, the experimentally measured forces were consistently identical to those predicted theoretically. These results correspond to a deformation distance of 2 mm into the tissue. If the pressure is held constant, varying the deformation distance (for example, between 0 and 5 mm) of the impactor tip into the biological material will not affect the transient force response, since the soft viscoelastic structure of the dura mater will provide a negligible amount of resistance to impact.

4 CONCLUSIONS

Following a review of the various test fixtures which have been used to simulate head impact injury, it is apparent that there is an inconsistency in defining the impact conditions and the experimental methods used in studying traumatic brain injuries. This paper has described the development of an experimental device which can be used to simulate the occurrence of traumatic brain injury in a controlled and systematic manner. Particular regard was given to the type of impact and the biomechanical response, i.e., whether it was due to linear or rotational accelerations, or combinations thereof, and whether the head underwent these accelerations due to the action of direct or indirect forces.

Direct cranial impact devices were seen to be prone to large variability in the injury response because of the difficulty in controlling the dynamic response of the head and the impactor-skull interface. Moreover, unrestrained skull impact experiments are believed [28] to always produce combined linear and rotational accelerations of the head and complete head constraint is difficult to effect in skull impact experiments. The objective of the present work has been to develop a device which can produce controlled injuries solely as a result of linear accelerations and consequently it was concluded that a direct brain impact device would be more appropriate in this respect. A rigid body brain impact device was considered to be more suitable than either a vacuum deformation or fluid percussion device since the brain deformations can be most easily related to biomechanical conditions when the impact velocity is carefully controlled. Dixon et al. [29] showed that the pressure pulse in a fluid percussion device does not apply a simple load form to the intracranial contents and that such a method is difficult to analyse biomechanically since the fluid enters the calvarium and disperses diffusely within the extradural space. The vacuum deformation devices are similar but allow greater control of the magnitude, shape and duration of the pressure pulse. However, the resulting mechanism of injury in both the vacuum and fluid impact devices is dissimilar to closed head injury in humans where injury results from the brain impacting against the skull with accelerating-decelerating movements of the brain.

A controlled and versatile system of applying linear impacts to exposed dura mater *in-situ* was designed, manufactured and calibrated. The impact device is classified as a direct brain rigid body impact device. The device is conceptually similar to that used by Dixon et al. [29] and Cherian et al. [31] but is more versatile since it provides complete freedom to vary the

line of action of the impact while ensuring that the line of action passes through the centre of mass of the head, thereby avoiding the effects of any rotational accelerations. Impact conditions were calculated analytically and validated experimentally. This experimental device has been approved for use by the University Ethics Committee in conjunction with intracerebral microdialysis techniques in order to quantify various neurochemical responses of the brain during trauma. Future publications will present these results although preliminary findings are available in [56, 57]. While this device can be used to model a number of different traumatic lesions, it is likely that it will be of greatest use in simulating concussion, contusion and axonal injury, as indicated in Table 3.

Model	**Concussion**	**Axonal Injury**	**Brain Swelling**	**Contusion**	**ASDH**[a]	**ICH**[a]
Fluid Percussion						
Central	+++[b]	+	-	+	-	-
Lateral	+++	+	-	+	-	-
Rigid Indentation						
Central	+++	+	-	+	-	-
Lateral	++	+	-	+	-	-
Contralateral	++	++	-	+	-	-
Local Tensile	-	-	-	+++	-	-
Injection	-	-	-	-	+++	+
Inertial	+++	+++	-	±	++	-
Impact Acceleration	+++	++	-	+	-	-

[a] ASDH, acute subdural haematoma; ICH, intracerebral haematoma

[b] -, does not duplicate the condition; ±, inconstant; +, duplicates to some degree; ++, greater fidelity; +++, greatest fidelity.

Table 3: Biofidelity of various test methods (after Gennarelli, [58]).

ACKNOWLEDGEMENTS

The assistance provided by Mr Cian O'Cuilleanain and Mr Luke Curley is gratefully acknowledged.

REFERENCES

1. Holbourn, A.H.S. (1943) Mechanics of head injuries. *Lancet*, **2**, 438-441.
2. Goldsmith, W. (1970) Biomechanics of head injury. In: *Biomechanics, Its Foundation and Objective.* Edited by Y.C. Fung, N. Perrone and M. Anliker. Prentice-Hall, New Jersey, 585-634.
3. Smith, D.H. and Meaney, D.F. (2000) Axonal damage in traumatic brain injury. *The Neuroscientist*, **6**, 483-495.
4. Gennarelli, T.A. (1983) Head injury in man and experimental animals: clinical aspects. *Acta Neurochirurgica*, **Supplementum 32**, 1-13.
5. Gurdjian, E. S. and Gurdjian, E. (1975) Re-evaluation of the bio-mechanics of blunt impact injury of the head. *Surgery, Gynecology & Obstetrics*, **140**, 845-850.
6. Ommaya, A.K. and Gennarelli, T.A. (1974) Cerebral concussion and traumatic unconsiousness: Correlation of experimental and clinical observations on blunt head injuries. *Brain*, **97**, 633-654.
7. Pudenz, R.H. and Shelden, C.H. (1946) The Lucite calvarium – a method for direct observation of the brain, II. Cranial trauma and brain movement. *J. Neurosurg.*, **3**, 487-505.

8. Gennarelli, T.A. and Thibault, L.E. (1982) Biomechanics of acute subdural hematoma. *J. Trauma*, **22**, 680-686.
9. Stalhammar, D. (1986) Experimental models of brain injury. *Acta Neurochirurgica*, **Supplementum 36**: 33-46.
10. Viano, D.C. (1988) Biomechanics of head injury – toward a theory linking head dynamic motion, brain tissue deformation and neural trauma. *SAE Trans. Paper*, 881706, 1070-1089.
11. Krantz, K.P.G. and Loewenhielm, C.G.P. (1986) Head and neck injuries. *Acta Neurochirurgica*, **Supplementum 36**, 47-50.
12. Boström, K. and Helander, C.G. (1986) Aspects on pathology and neuropathology in head injury. *Acta Neurchirurgica*, **Supplementum 36**, 51-55.
13. Wilberger, J.E., Jr., Harris, M. and Diamond, D.L., (1990) Acute subdural hematoma: Morbidity and mortality relating to timing of operative intervention. *J. Trauma*, **30** (6), 733-736.
14. Nishimoto, T. and Murakami, S. (1998) Relation between diffuse axonal injury and internal head structures on blunt impact. *J. Biomech. Eng.*, **120**, 140-147.
15. Adams, J.H, Doyle, D. and Ford, I. (1989) Diffuse axonal injury in head injury: Definition, diagnosis and grading. *Histopathology*, **15**, 49-59.
16. Povlishock, J.T. (1993) Pathobiology of traumatically induced axonal injury in animals and man. *Ann. Emerg. Med.*, **22**, 980–986.
17. Gilchrist, M.D. and O'Donoghue, D. (2000) Simulation of the development of frontal head impact injury. *Computational Mechanics*, **26**, 229-235.
18. Gilchrist, M.D., O'Donoghue, D. and Horgan, T. (2001) A two dimensional analysis of the biomechanics of frontal and occipital head impact injuries. *Int. J. Crashworthiness*, **6**, 253-262.
19. Gilchrist, M.D. (2003) Modelling and accident reconstruction of head impact injuries. *Key Engng Materials*, **245-246**, 417-430.
20. O'Riordain, K., Thomas, P.M., Phillips, J.P. and Gilchrist, M.D. (2003) Reconstruction of real world head injury accidents resulting from falls using multibody dynamics. *J. Clin. Biomechanics*, **18**, 590-600.
21. Horgan, T.J. and Gilchrist, M.D. (2003) The creation of three-dimensional finite element models for simulating head impact biomechanics. *Int. J. Crashworthiness*, **8**, 353-366.
22. Horgan, T.J. and Gilchrist, M.D. (2004) Influence of FE model variability in predicting brain motion and intracranial pressure changes in head impact simulations. *Int. J. Crashworthiness*, **9**, in press.
23. King, A.I. and Viano, D.C. (1995) Mechanics of head/neck. In: *The Biomedical Engineering Handbook*. CRC Press, Boca Raton, FL.
24. Feeney, D.M., Boyson, M.G., Linn, R.T., Murray, H.M. and Dail, W.G. (1981) Responses to cortical injury, Part I. *Brain Res.*, **211**, 67-77.
25. Koizumi, H., Fujisawa, H., Ito, H., Maekawa, T., Di, X. and Bullock, R. (1997) Effects of mild hypothermia on cerebral blood flow-independent changes in cortical extracellular levels of amino acids following contusion trauma in the rat. *Brain Research*, **747**, 304-312.
26. Lighthall, J.W. (1988) Controlled cortical impact: A new experimental brain injury model. *J. Neurotrauma*, **5**, 1-15.
27. Anderson, T.E. (1982) A controlled pneumatic technique for experimental spinal cord contusion. *J. Neurosci. Methods*, **6**, 327-333.
28. Lighthall, J.W., Dixon, C.E., Anderson, T.E. (1989) Experimental models of brain injury. *J. Neurotrauma*, **6**, 83-97.
29. Dixon, C.E., Clifton, G.L., Lighthall, J.W., Yaghmai, A.A. and Hayes, R.L. (1991) A controlled cortical impact model of traumatic brain injury in the rat. *J. Neurosci. Methods*, **39**, 253-262.
30. Baldwin, S.A., Fugaccia, I. and Brown, D.R. (1996) Blood brain barrier breach following cortical contusion in the rat. *J. Neurosurg.*, **85**, 476-481.
31. Cherian, L., Robertson, C. S., Contant, C. F. Jr. and Bryan, R. M. Jr. (1994) Lateral cortical impact injury in rats. *J. Neurotrauma*, **11**, 573-585.
32. Shreiber, D.I., Bain, A.C., Ross, D.T., Smith, D.H., Gennarelli, T.A., McIntosh, T.K. and Meaney, D.F. (1999) Experimental investigation of cerebral contusion: Histopathological and immunohistochemical evaluation of dynamic cortical deformation. *J. Neuropath. Exp. Neurol.*, **58**, 153-164.
33. Shreiber, D.I., Smith, D.H. and Meaney, D.F. (1999) Immediate in vivo response of the cortex and the blood-brain barrier following dynamic cortical deformation in the rat. *Neurosci. Letters*, **259**, 5-8.
34. Murai, I.I., Nakamura, T. and Tamaura, A. (1991) Localised cerebral contusion model. *Proc. 1st Int. Neurotrauma Symp.*, Fukishima, Japan.

35. Mathew, P., Graham, D.I., Bullock, R., Maxwell, W., McCulloch, J. and Teasdale, G. (1994) Focal brain injury: histological evidence of delayed inflammatory response in a new rodent model of focal cortical injury. *Acta Neurochir.*, **Supplement 60**, 428-430.
36. Mathew, P., Bullock, R., Graham, D.I., Maxwell, W.L., Teasdale, G.M. and McCulloch, J. (1996) A new experimental model of contusion in the rat: Histopathological analysis and temporal patterns of cerebral blood flow disturbances. *J. Neurosurg.*, **85**, 860-870.
37. Lindgren, S. and Rinder, L. (1969) Production and distribution of intracranial and intraspinal pressure changes at sudden extradural fluid volume input in rabbits. *Acta Physiol Scand*, **76**, 340-351.
38. Sullivan, H.G., Martinez, J., Becker, D.P., Miller, J.D., Griffith, R. and Wist, A.O. (1976) Fluid percussion of mechanical brain injury in the cat. *J. Neurosurg.*, **45**, 520-534.
39. Povlishock, J.T., Becker, D.P., Cheng, C.L.Y. and Vaughan, G.W. (1983) Axonal change in minor head injury. *J. Neuropathol. Exp. Neurol.*, **42**, 225-242.
40. Dixon, C.E., Lyeth, B.G. and Povlishock, J.T. (1987) A fluid percussion model of experimental brain injury in the rat: neurological, physiological, and histopathological characterizations. *J. Neurosurg.*, **67**, 110-119.
41. McIntosh, T.K., Vink, R., Noble, L., Yamakami, I., Fernyak, S., Soares, H., Faden, A.L. (1989) Traumatic brain injury in the rat: Characterization of a lateral fluid-percussion model. *Neuroscience*, **28**, 233-244.
42. Yamaki, T., Murakami, N., Iwamoto, Y., Yoshino, E., Nakagawa, Y., Ueda, S., Horikawa, J. and Tsujii, T. (1994) A modified fluid percussion device. *J. Neurotrauma*, **11**, 613-622.
43. Denny-Brown, D. and Russell, W.R. (1941) Experimental cerebral concussion. *Brain*, **64**, 93-164.
44. Nilsson, B., Ponten, U. and Voigt, G. (1978) Experimental head injury in the rat. Part I: Mechanics, pathophysiology, and morphology in an impact acceleration trauma. *J. Neurosurg.*, **47**, 241-251.
45. Madsen, F.F. and Reske-Nielsen, E. (1987) A simple mechanical model using a piston to produce localised cerebral contusions in pigs. *Acta Neurochir. (Wien)*, **88**, 65-72.
46. Marmarou, A., Foda M.A.A., Van den Brink, W., Campbell, J., Kita, H. and Demetriadou, K. (1994) A new model of diffuse brain injury in rats. Part I: Pathophysiology and biomechanics. *J. Neurosurg.*, **80**, 291-300.
47. Shapira, Y., Shohami, E. and Sidi, A. (1988) Experimental closed head injury in rats: mechanical, pathophysiologic, and neurologic properties. *Crit. Care Med.*, **16**, 258- 265.
48. Adelson, P.D., Robichaud, P., Hamilton, R.L. and Kochanek, P.M. (1996) A model of diffuse traumatic brain injury in the immature rat. *J. Neurosurg.*, **85**, 877-884.
49. Park, H.K., Fernandez, I., Dujovny, M. and Diaz, F.G. (1999) Experimental animal models of traumatic brain injury. *Crit. Rev. Neurosurg.*, **9**, 44-52.
50. Harris, G.F., Yoganandan, N., Schmaltz, D., Reinartz, J., Pintar, F. and Sances, A. (1993) A biomechanical impact test system for head and facial injury assessment and model development. *J. Biomed. Eng.*, **15**, 67-73.
51. Goldman, H., Hodgson, V. and Morehead, M. (1991) Cerebrovascular changes in a rat model of moderate closed-head injury. *J. Neurotrauma*, **8**, 129-144.
52. Parkinson, D., West, M. and Pathiraja ,T. (1978) Concussion: Comparison of humans and rats. *J. Neurosurg.*, **3**, 176-180.
53. Beckman, D.L. and Bean, J.W. (1969) Pulmonary damage and head injury. *Proc. Soc. Exp. Biol. Med.*, **130**, 5-9.
54. Bakay, L., Lee, J.C. and Lee, G.C. (1989) Experimental cerebral concussion. Part I: An electron microscopic study. *J. Neurosurg.*, **47**, 525-531.
55. West, M., Parkinson D. and Havlicek, V. (1982) Spectral analysis of the electroencephalographic response to experimental concussion in the rat. *Electroencephalogr. Clin. Neurophysiol.*, **53**, 192-200.
56. Smyth, A., Gallagher, C., Gilchrist, M.D. and O'Connor, W.T. (2003) Development of a microdialysis model of traumatic brain injury. Proceedings of the 33rd Annual Neuroscience Meeting, New Orleans, USA, Nov 8-12.
57. Smyth, A., Gilchrist, M.D., Earley, B. and O'Connor, W.T. (2004) Traumatic brain injury to the medial prefrontal cortex differentially affects local dialysate glutamate, aspartate and GABA levels in the rat. Proceedings of the 34th Annual Neuroscience Meeting, San Diego, USA, Oct 23-27.
58. Gennarelli, T.A. (1994) Animate models of human head injury. *J. Neurotrauma*, **11**, 357-368.

Figure 1: Loading response associated with A: short, B: medium and C: long duration impacts. Shaded area represents loading and dashed line represents response. Reproduced with permission from [9].

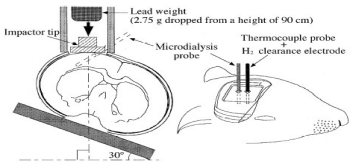

Figure 2: Weight drop device of Koizumi et al. [25] (reproduced with permission).

Figure 3: Controlled cortical impact experiments of Cherian et al. [31] (reproduced with permission).

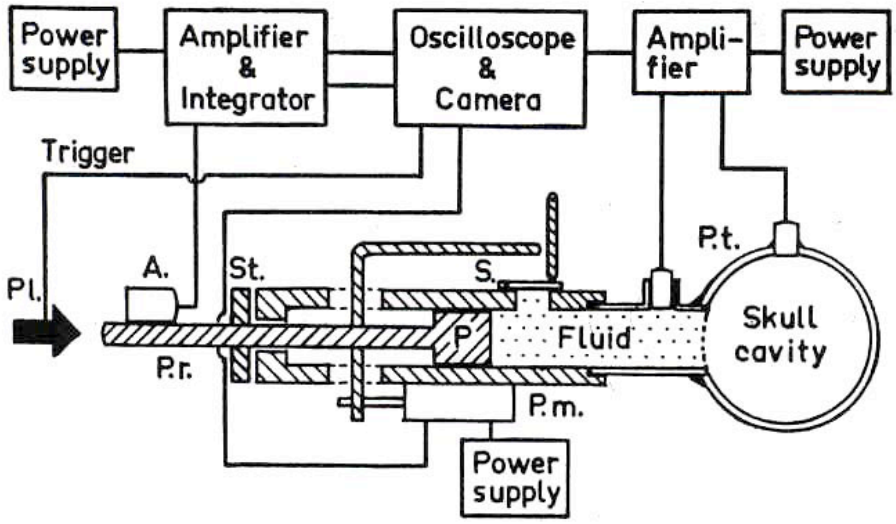

Figure 4: Schematic setup of fluid percussion experiments. Reproduced with permission from [37].

Figure 5: Modified fluidic impact device used by Yamaki et al. [42] (reproduced with permission).

Figure 6: DAI by weight drop. Reproduced with permission from [46].

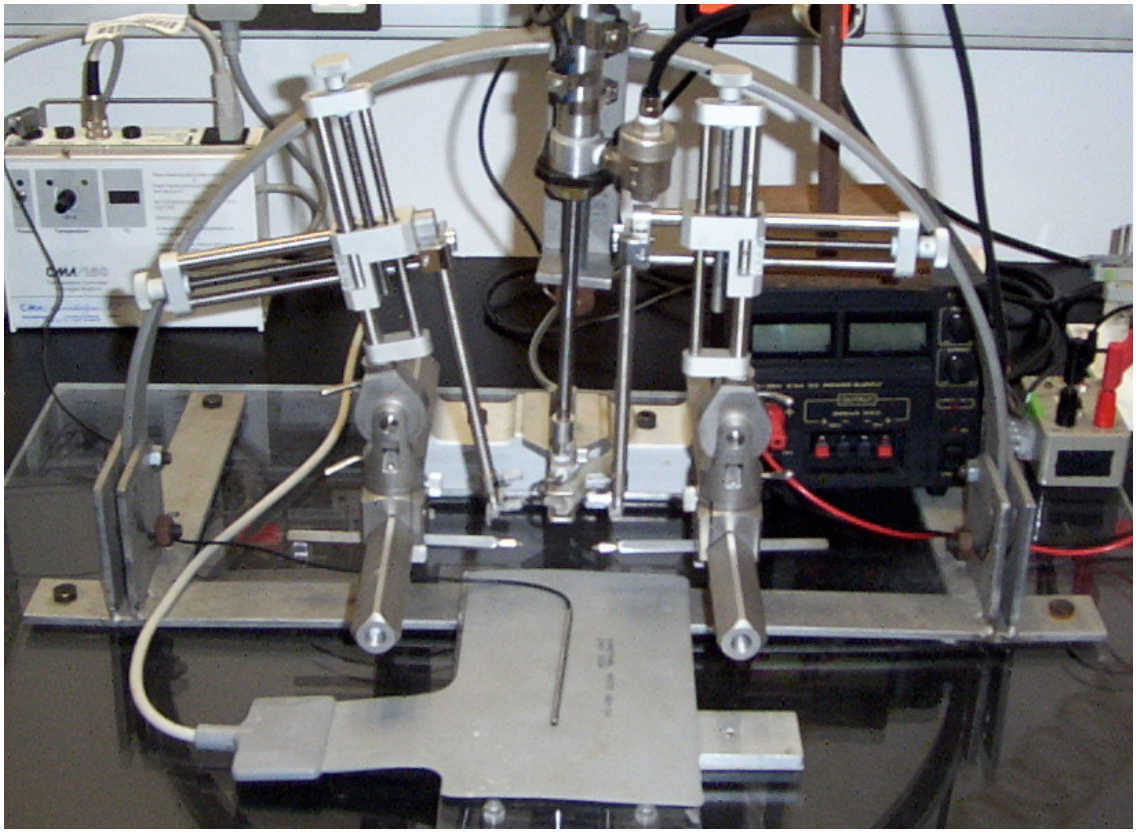

Figure 7: Linear impact device showing how line of action of impact can be varied in two degrees of freedom. The impact device is connected to a stereotaxic frame. A hemispherical indenter tip is attached to the end of the linear actuator.

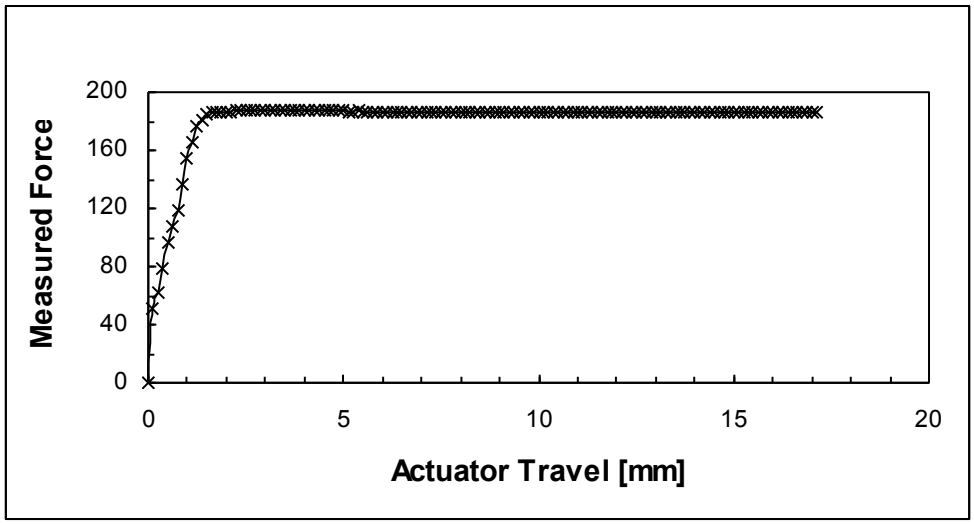

Figure 8: Measured force applied by actuator impactor for a gauge pressure of 60 kPa. Note that the maximum force of 187.9 N occurs after 3 mm of travel and this force reduces to 185.2 N at the full actuator extension of 125 mm (not shown). Thus, the quasi-static force is 185.2 N and the inertial force is 2.7 N (= 187.9 – 185.2).